Indian Journal of Pure & Applied Physics
Vol. 58, February 2020, pp. 71-78

Numerical investigation of unsteady MHD flow and radiation heat transfer past a stretching surface in porous media with viscous dissipation and heat generation/absorption

Susheela Chaudhary[a], Santosh Chaudhary[b*] & Mohan Kumar Choudhary[b]

[a]Department of Mathematics, Government Science College, Sikar 332 001, India

[b]Department of Mathematics, Malaviya National Institute of Technology, Jaipur 302 017, India

Received 31 March 2019; accepted 2 January 2020

Viscous dissipation and radiation effects on unsteady flow of laminar incompressible viscous electrically conducting fluid through stretching surface in a porous media with magnetic field and heat generation/absorption have been investigated. Taking suitable similarity variables, the governing boundary layer equations are converted into a set of ordinary differential equations and solved numerically by Runge-Kutta fourth order method along with shooting technique. The effects of the various physical dimensionless parameters such as unsteadiness parameter, permeability parameter, magnetic parameter, radiation parameter, Prandtl number, heat generation/absorption parameters and Eckert number for velocity and temperature distributions have been analyzed in detail through graphical representations. Further skin friction coefficient and Nusselt number at the surface are numerated and compared with previous researchers.

Keywords: Unsteady MHD flow, Radiation, Stretching surface, Porous media, Viscous dissipation, Heat generation/absorption

1 Introduction

Magnetohydrodynamics (MHD) is related to the study of the motion of electrically conducting fluids and their interactions with magnetic fields. MHD flows toward a stretching sheet have been attracted a great attention in the past few decades because of its increasing applications in industrial and technological processes such as annealing and spinning of metal wires, drawing and extrusion of plastic and rubber sheets, packed bed reactors, glass blowing, hot rolling and the enhanced recovery of petroleum resources. The mixture issued from a slit is subsequently stretched in all of the above mentioned engineering processes to get the desired thickness. Crane[1] was the first who found an analytical solution for the steady two-dimensional flow on a linearly stretched surface in a quiescent incompressible fluid. Later, many researchers like Andersson *et al.*[2], Ariel[3], Elbashbeshy and Bazid[4], Kelson[5], Das[6], Khan *et al.*[7] and Chaudhary *et al.*[8] have presented various aspects of stretching sheet problems for non-magnetic and magnetic cases.

Porous material is a solid permeated by an interconnected network of pores filled with a fluid. Many natural matters like soils, rocks, bones and manmade substances, for example cement, foams and ceramics can be considered as porous media. Fluid flow through porous medium is a subject to most common interest and has emerged a separate field of study because of its vast importance in numerous technological applications such as geothermal systems, grain storage, heat exchangers, catalytic reactors, metal processing, etc. Following the work of Vafai and Kim[9], many researchers like Ishak *et al.*[10], Rosali *et al.*[11] and Chaudhary and Kumar[12] have considered various aspects of heat transfer problem in porous medium and obtained similarity solutions. Furthermore, Chaudhary and Choudhary[13], and Shit *et al.*[14] presented an excellent review of boundary layer flow with porous medium and some related applications.

Heat transfer in the boundary layer flow of participating fluid is significantly affected by thermal radiation especially at high absolute temperature levels. All bodies emit energy continuously due to their temperature, and thus emitted energy is called thermal radiation. This process is very useful in space technology and also very important in various practical applications namely engines integrated circuit and it's cooling, cooling of nuclear reactors, propulsion devices, design of reliable equipments of

*Corresponding author (E-mail: d11.santosh@yahoo.com)

space vehicles and aircrafts, plasmas, turbines, satellites and missiles. The thermal radiation effects on the flow with and without a magnetic field with several cases were presented by Bestman and Adjepong[15], Makinde and Ogulu[16], Pal and Mondal[17], and Jat and Chaudhary[18]. Some other studies have been carried out by Chaudhary *et al*.[19], Sandeep *et al*.[20] and Chaudhary and Choudhary[21] with thermal radiation heat transfer under the different configurations.

Inspired by the research work of Elbashbeshy and Emam[22], the main objective of this paper is to study the magnetohydrodynamic effects on viscous incompressible fluid and heat transfer in the presence of viscous dissipation and radiation effects with heat generation or absorption.

2 Mathematical Analysis

Consider two-dimensional unsteady flow of a viscous incompressible electrically conducting fluid and heat transfer due to radiation over a stretching sheet in a porous medium with heat generation/absorption. Cartesian coordinate system (X,Y) is assumed where the $X-$ and $Y-$axes are taken along the directions of stretching surface and normal to it, respectively. A uniform transverse magnetic field of constant strength B_0 is also assumed, as shown in Fig. 1. The magnetic Reynolds number is taken sufficiently small to neglect of the induced magnetic field. The surface is stretched with linear velocity $U_w = \frac{ax}{1-bt}$ and temperature of the sheet is $T_w = T_\infty + \frac{a}{2\upsilon x^2}\frac{1}{(1-bt)^{3/2}}$ where, a is the positive constant, b is the rate of stretching, t is the time, T_∞ is the free stream temperature and υ is the kinematic viscosity. The following three equations represent the equation of continuity, momentum and energy, respectively.

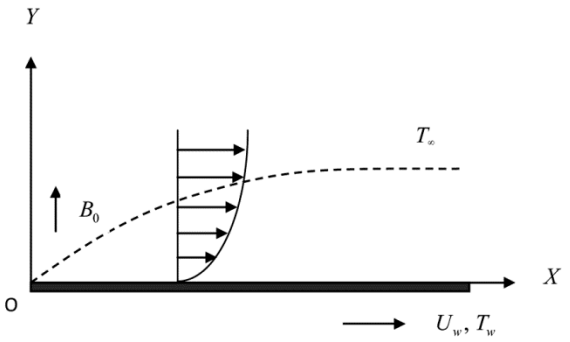

Fig. 1 – Schematic of the physical system.

$$\frac{\partial u}{\partial x}+\frac{\partial v}{\partial y}=0 \quad \text{... (1)}$$

$$\frac{\partial u}{\partial t}+u\frac{\partial u}{\partial x}+v\frac{\partial u}{\partial y}=\upsilon\frac{\partial^2 u}{\partial y^2}-\left(\frac{\upsilon}{K}+\frac{\sigma_e {B_0}^2}{\rho}\right)u \quad \text{... (2)}$$

$$\rho C_p\left(\frac{\partial T}{\partial t}+u\frac{\partial T}{\partial x}+v\frac{\partial T}{\partial y}\right)=\kappa\frac{\partial^2 T}{\partial y^2}-\frac{\partial q_r}{\partial y}+Q(T-T_\infty)+\mu\left(\frac{\partial u}{\partial y}\right)^2 \quad \text{... (3)}$$

Subject to the boundary conditions:

$$\begin{aligned} &y=0 \quad : \quad u=U_w,\ v=0,\ T=T_w \\ &y\to\infty : \quad u\to 0,\ T\to T_\infty \end{aligned} \quad \text{... (4)}$$

where, u and v are the components of velocity in the x and y directions, respectively, K is the permeability, σ_e is the electrical conductivity, ρ is the fluid density, C_p is the specific heat at constant pressure, T is the temperature of the fluid, κ is the thermal conductivity, q_r is the radiative heat flux, Q is the heat source when $Q>0$ or heat sink when $Q<0$ and μ is the coefficient of fluid viscosity.

The radiative heat flux is simplified by using the Rosseland approximation for radiation as (Brewster[23]):

$$q_r=-\frac{4\sigma^*}{3k^*}\frac{\partial T^4}{\partial y} \quad \text{... (5)}$$

where, σ^* and k^* are the Stefan-Boltzmann constant and the absorption coefficient, respectively.

Assuming that there is a temperature differences within the flow, such the term T^4 may be expressed as a linear function of temperature by using Taylor series about T_∞ and neglecting higher order terms:

$$T^4 \cong 4{T_\infty}^3 T-3{T_\infty}^4 \quad \text{... (6)}$$

Using Eqs (5) and (6), the Eq. (3) can be written as:

$$\rho C_p\left(\frac{\partial T}{\partial t}+u\frac{\partial T}{\partial x}+v\frac{\partial T}{\partial y}\right)=\kappa\frac{\partial^2 T}{\partial y^2}+\frac{16\sigma^*{T_\infty}^3}{3k^*}\frac{\partial^2 T}{\partial y^2}+Q(T-T_\infty)+\mu\left(\frac{\partial u}{\partial y}\right)^2 \quad \text{... (7)}$$

Using the standard definition of stream function such as $u = \partial\psi/\partial y$ and $v = -\partial\psi/\partial x$, the following similarity transformations (Elbashbeshy and Emam[22]) are introduced:

$$\eta = y\left[\frac{a}{\upsilon(1-bt)}\right]^{1/2},\ \psi(x,y,t) = \left[\frac{a\upsilon}{(1-bt)}\right]^{1/2} xf(\eta),$$

$$\theta(\eta) = \frac{T - T_\infty}{T_w - T_\infty} \qquad \text{... (8)}$$

where, η is the similarity variable, and $f(\eta)$ and $\theta(\eta)$ are the dimensionless stream function and temperature, respectively. The Eqs (2) and (7) are converted into:

$$f''' + f\,f'' - f'^2 - A\left(\frac{1}{2}\eta\,f'' + f'\right) - (\lambda + M)\,f' = 0 \qquad \text{... (9)}$$

$$\left(1 + \frac{4}{3R}\right)\theta'' + \Pr\left[f\theta' - \frac{A}{2}(\eta\theta' + 3\theta) + (\delta + 2f')\theta + Ecf''^2\right] = 0 \qquad \text{... (10)}$$

with the transformed boundary conditions:

$$\begin{aligned} &\eta = 0 :\ f = 0,\ f' = 1,\ \theta = 1 \\ &\eta \to \infty :\ f' \to 0,\ \theta \to 0 \end{aligned} \qquad \text{... (11)}$$

where, primes denote differentiation with respect to η. $A = \dfrac{b}{a}$ is the unsteadiness parameter, $\lambda = \dfrac{\upsilon^2 \operatorname{Re}_x}{KU_w^{\,2}}$ is the permeability parameter, $\operatorname{Re}_x = \dfrac{U_w x}{\upsilon}$ is the local Reynolds number, $M = \dfrac{\upsilon\sigma_e B_0^{\,2} \operatorname{Re}_x}{\rho U_w^{\,2}}$ is the magnetic parameter, $R = \dfrac{\kappa k^*}{4\sigma^* T_\infty^{\,3}}$ is the thermal radiation parameter, $\Pr = \dfrac{\mu C_p}{\kappa}$ is the Prandtl number, $\delta = \dfrac{Q\upsilon^2 \operatorname{Re}_x}{\mu C_p U_w^{\,2}}$ is the heat source/sink parameter and $Ec = \dfrac{U_w^{\,2}}{C_p(T_w - T_\infty)}$ is the Eckert number.

In practical applications, the quantities of physical interest are the skin friction coefficient C_f and the Nusselt number Nu_x, which are defined as:

$$C_f = 2\operatorname{Re}_x^{\,-1/2} f''(0) \qquad \text{... (12)}$$

$$Nu_x = -\operatorname{Re}_x^{\,1/2}\,\theta'(0) \qquad \text{... (13)}$$

3 Solution Procedures

Equations (9) and (10) with the boundary conditions (11) are solved numerically by Runge-Kutta fourth order method along with shooting technique. Introducing the new set of variables p_1, p_2, p_3, q_1 and q_2, the following set of linear differential equations of first order are obtained

$$p_1' = p_2 \qquad \text{... (14)}$$

$$p_2' = p_3 \qquad \text{... (15)}$$

$$p_3' = -\left[p_1 p_3 - A\left(\frac{1}{2}\eta\,p_3 + p_2\right) - p_2^{\,2} - (M + \lambda)p_2\right] \qquad \text{... (16)}$$

and

$$q_1' = q_2 \qquad \text{... (17)}$$

$$q_2' = -\left(\frac{3R}{4 + 3R}\right)\Pr\left[p_1 q_2 - \frac{A}{2}(\eta\,q_2 + 3q_1) + (2p_2 + \delta)q_1 + Ecp_3^{\,2}\right] \qquad \text{... (18)}$$

with the boundary conditions

$$\begin{aligned} &\eta = 0 :\ p_1 = 0,\ p_2 = 1,\ q_1 = 1 \\ &\eta \to \infty :\ p_2 \to 0,\ q_1 \to 0 \end{aligned} \qquad \text{... (19)}$$

where, $p_1 = f$ and $q_1 = \theta$.

In order to solve Eqs (16) and (18) with the boundary conditions (19) by Runge-Kutta method the values for p_3 and q_2 are required at the surface. So the initial guesses values for $p_3(0)$ and $q_2(0)$ are chosen and Runge-Kutta method of fourth order is applied taking the step size $\Delta\eta = 0.001$. Comparing the estimated values of p_2 and q_1 for different values of various parameters at the far field boundary condition $\eta \to \infty \approx 6$ (say) with the given boundary conditions $p_2(6) \to 0$ and $q_1(6) \to 0$, the values of $p_3(0)$ and $q_2(0)$ are improved accordingly from the initial values to give an approximate solution. The

process is repeated until the results converge to six places of decimals.

4 Validation

This section is devoted to validate the computational method which was applied in the previous section. The results of velocity gradient $f''(0)$ and heat transfer rate $\theta'(0)$ for different values of governing parameters are compared in the limiting cases with the previous published work of Elbashbeshy and Emam[22] in Table 1. From this table, it is noteworthy that the present results are in excellent agreement.

5 Results and Discussion

In order to get clear insight of the considered model, the results of velocity $f'(\eta)$ and temperature $\theta(\eta)$ for various parameters like the unsteadiness parameter A, the permeability parameter λ, the magnetic parameter M, the thermal radiation parameter R, the Prandtl number $\Pr$, the heat source/sink parameter δ and the Eckert number Ec are plotted through graphs, while the other parameters are taken constant. Further, the values of $f''(0)$ and $\theta'(0)$ which are proportional to local skin friction coefficient C_f and local Nusselt number Nu_x, respectively have been numerated through table.

Effects of the unsteadiness parameter A on the fluid velocity $f'(\eta)$ and the temperature $\theta(\eta)$ have been demonstrated in Figs 2 and 3, respectively, taking other parameters constant. It may be observed that the velocity and the temperature decrease faster with the increasing values of the unsteadiness parameter A while the reverse phenomenon occurs for $\eta > 3$ in Fig. 2. This is due to the fact that the thermal boundary layer thickness decreases faster when unsteadiness parameter increases before $\eta \approx 3$ but ultimately it increases the velocity of the fluid.

Figures 4 and 5 present the velocity $f'(\eta)$ and temperature $\theta(\eta)$ for different values of the permeability parameter λ, respectively, keeping other parameters constant. It is noteworthy that the velocity and the temperature decrease with the increasing values of the permeability parameter λ. The actual

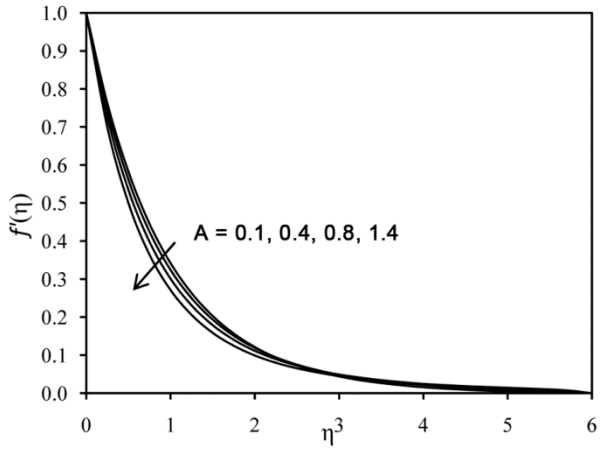

Fig. 2 – Variation of the velocity for different values of A with $\lambda = 0.1$ and $M = 0.01$.

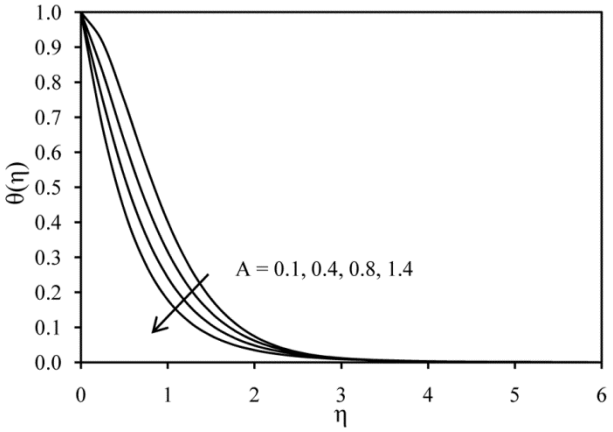

Fig. 3 – Variation of the temperature for different values of A with $\lambda = 0.1, M = 0.01,\ R = 0.3, \Pr = 10, \delta = -0.5$ and $Ec = 0.01$.

Table 1 – Comparison of $f''(0)$ and $\theta'(0)$ for various values of $A, \lambda, R, \Pr$ and δ with $M = Ec = 0.0$.

A	λ	R	$\Pr$	δ	$-f''(0)$		$-\theta'(0)$	
					Elbashbeshy and Emam[22]	Present result	Elbashbeshy and Emam[22]	Present result
0.4	0.1	0.3	10	-0.5	1.17853	1.178629	0.53765	0.537818
0.8					1.30035	1.300447	0.98601	0.986231
	0.3				1.37550	1.375596	1.00056	1.000777
	0.5				1.44668	1.446767	1.01364	1.013854
	0.7				1.51445	1.514543	1.02552	1.025732

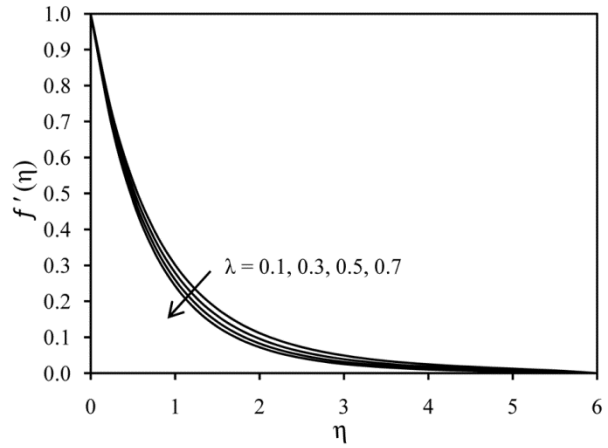

Fig. 4 – Variation of the velocity for different values of λ with $A = 0.8$ and $M = 0.01$.

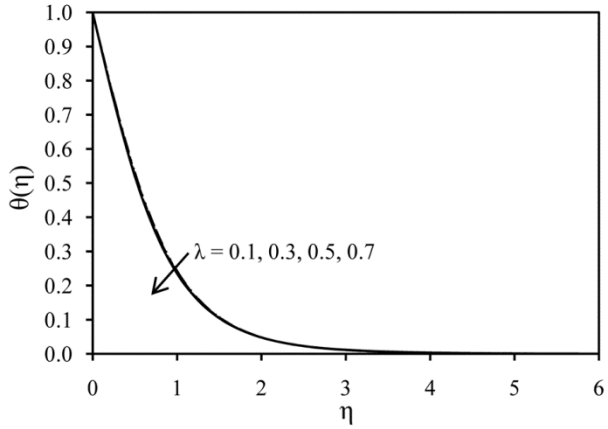

Fig. 5 – Variation of the temperature for different values of λ with $A = 0.8, M = 0.01, R = 0.3, \Pr = 10, \delta = -0.5$ and $Ec = 0.01$.

effect of the permeability parameter is to make the velocity and temperature distribution more uniform within the boundary layer. So, it can be effectively used for the fast cooling of the sheet.

Effects of the magnetic parameter M on the velocity $f'(\eta)$ and the temperature $\theta(\eta)$ profiles have been plotted in Figs 6 and 7, respectively, while the other parameters are constant. From these figures it is evident that the velocity decreases with the increasing values of the magnetic parameter M but the reverse phenomena occurs for the temperature distribution. The application of a uniform magnetic field normal to the flow direction gives rise to Lorentz force which acts in the negative direction of flow. This force has tendency to slow down the movement of the fluid and enhances its temperature.

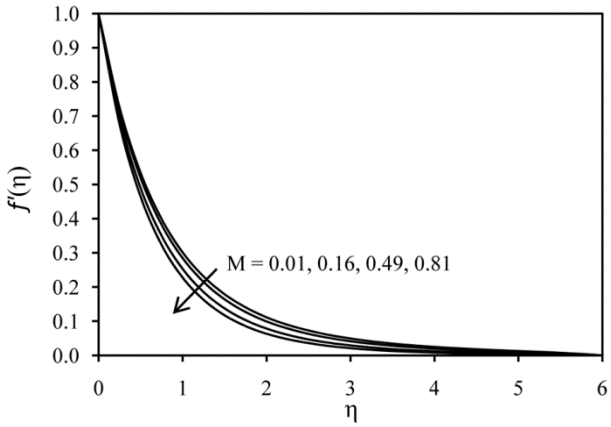

Fig. 6 – Variation of the velocity for different values of M with $A = 0.8$ and $\lambda = 0.1$.

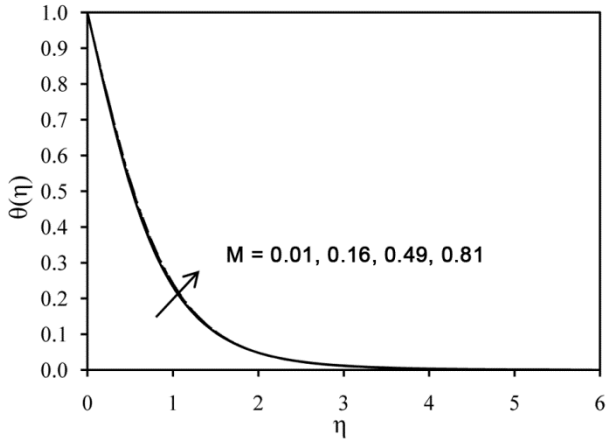

Fig. 7 – Variation of the temperature for different values of M with $A = 0.8, \lambda = 0.1, R = 0.3, \Pr = 10, \delta = -0.5$ and $Ec = 0.01$.

Influences of several values of the thermal radiation parameter R and the Prandtl number $\Pr$ on the temperature $\theta(\eta)$ distribution are displayed in Figs 8 and 9 when the other parameters are kept constant. It can be seen that the increase in thermal radiation parameter R and the Prandtl number $\Pr$ causes the decrease in the temperature profile. From a physical point of view, the fluid with a higher value of the Prandtl number posses a large heat capacity, and hence intensifies the heat transfer while, a smaller Prandtl number increases the thermal conductivity and therefore heat is able to diffuse away from the surface.

In Figs 10 and 11, the consequences of the variation in the heat source/sink parameter δ and the Eckert number Ec on the temperature $\theta(\eta)$ profiles

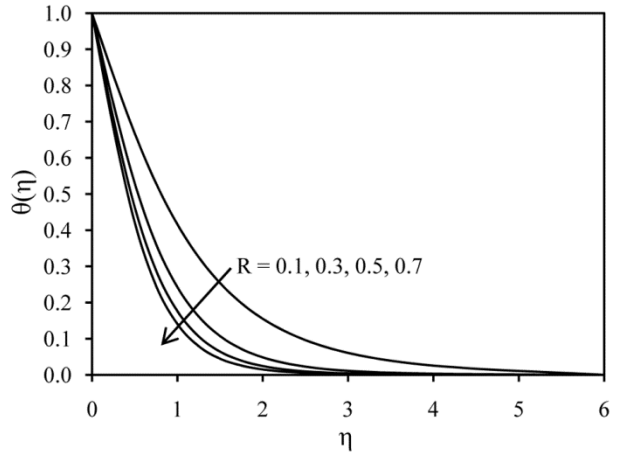

Fig. 8 – Variation of the temperature for different values of R with $A = 0.8, \lambda = 0.1,\ M = 0.01, \Pr = 10, \delta = -0.5$ and $Ec = 0.01$.

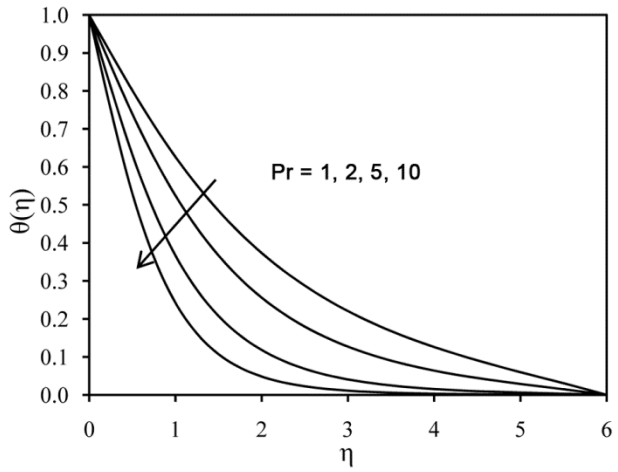

Fig. 9 – Variation of the temperature for different values of Pr with $A = 0.8, \lambda = 0.1,\ M = 0.01, R = 0.3, \delta = -0.5$ and $Ec = 0.01$.

are shown taking other parameters constant. It is noticed that both the parameters has an increasing effect on the temperature profiles. This is a consequence of the fact that for higher values of the Eckert number, there is significant generation of heat due to viscous dissipation near the sheet. Therefore, viscous dissipation in a flow through permeable surface is beneficial for gaining the temperature.

The numerical results for the local skin friction coefficient $f''(0)$ and the heat flux $\theta'(0)$ are tabulated in Table 2 for various values of the unsteadiness parameter A, the permeability parameter λ, the magnetic parameter M, the thermal radiation

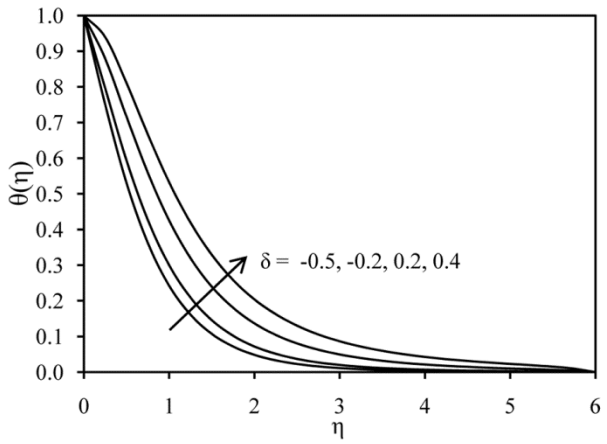

Fig. 10 – Variation of the temperature for different values of δ with $A = 0.8, \lambda = 0.1,\ M = 0.01, R = 0.3, \Pr = 10$ and $Ec = 0.01$.

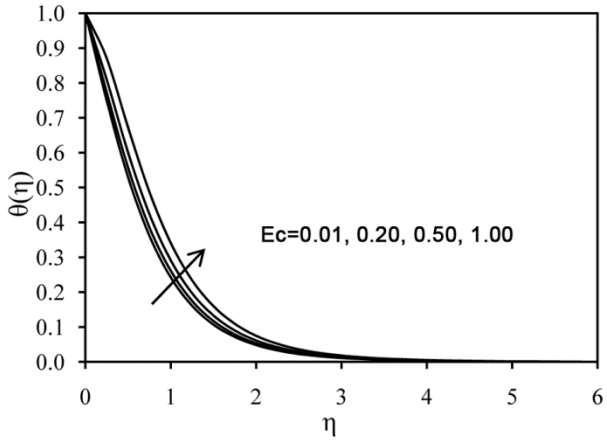

Fig. 11 – Variation of the temperature for different values of Ec with $A = 0.8, \lambda = 0.1,\ M = 0.01, R = 0.3, \Pr = 10$ and $\delta = -0.5$.

parameter R, the Prandtl number $\Pr$, the heat source/sink parameter δ and the Eckert number Ec. From this table it is observed that the local skin friction coefficient $f''(0)$ and the local Nusselt number $\theta'(0)$ decrease with the increasing values of the unsteadiness parameter A, the permeability parameter λ and the magnetic parameter M, keeping other parameters constant. Moreover, the local Nusselt number $\theta'(0)$ decreases with the increasing values of the thermal radiation parameter R and the Prandtl number $\Pr$, while the opposite phenomenon occurs for the heat source/sink parameter δ and the Eckert number Ec, keeping other

Table 2 – Numerical value of $f''(0)$ and $\theta'(0)$ for various value of considered parameters.

A	λ	M	R	Pr	δ	Ec	$-f''(0)$	$-\theta'(0)$
0.1	0.1	0.01	0.3	10	-0.5	0.01	1.086651	0.079819
0.4							1.182905	0.530843
0.8							1.304310	0.978970
1.4							1.470799	1.479770
0.8	0.3						1.379243	0.992822
	0.5						1.450232	1.005251
	0.7						1.517851	1.016517
	0.1	0.16					1.360906	0.988761
		0.49					1.477657	1.007664
		0.81					1.582545	1.023322
		0.01	0.1					0.676543
			0.5					1.135283
			0.7					1.238181
			0.3	1				0.399894
				2				0.526163
				5				0.752245
				10	-0.2			0.731654
					0.2			0.305716
					0.4			0.012615
					-0.5	0.20		0.826434
						0.50		0.585588
						1.00		0.184178

parameters constant. Further, it is observed that the values of the local skin friction coefficient $f''(0)$ are always negative for all the values of physical parameters considered. Physically, positive sign of skin friction coefficient $f''(0)$ implies that the fluid exerts a drag force on the sheet and negative sign implies the opposite meaning. It is also evident that the Nusselt number $\theta'(0)$ is negative for all the values of physical parameters considered, which means that there is a heat flow from the wall.

6 Conclusions

A numerical approach was applied to simulate the problem of the flow and heat transfer of two dimensional boundary layer flow of an electrically conducting fluid towards an unsteady stretching surface in porous medium in the presence of magnetic field and viscous dissipation. Several conclusions can be drawn from the results of this study:

(i) The velocity and the wall shear stress decrease with the rising values of the unsteadiness parameter, the permeability parameter and the magnetic parameter. Thereafter, the velocity enhances with an increment in the value of the unsteadiness parameter for eta greater than three and (ii) The temperature and the local Nusselt number reduce with the exciting values of the unsteadiness parameter, the permeability parameter, the magnetic parameter, the thermal radiation parameter and the Prandtl number, while reverse is true in the temperature field for the values of the magnetic parameter. Moreover, the thermal boundary layer as well as the surface heat flux developed along to the enlarging values of the heat source/sink parameter and the Eckert number.

References

1 Crane L J, *Z Angew Math Phys*, 21 (1970) 645.
2 Andersson H I, Aarseth J B & Dandapat B S, *Int J Heat Mass Trans*, 43 (2000) 69.
3 Ariel P D, *J Appl Math Mech*, 83 (2003) 844
4 Elbashbeshy E M A & Bazid M A A, *Heat Mass Trans*, 41 (2004) 1.
5 Kelson N A, *Int J Non-Linear Mech*, 46 (2011) 1090.
6 Das K, *Therm Sci*, 18 (2014) S475.
7 Khan M I, Tamoor M, Hayat T & Alsaedi A, *Results Phys*, 7 (2017) 1207.
8 Chaudhary S, Kanika KM & Choudhary M K, *Indian J Pure Appl Phys*, 56 (2018) 931.
9 Vafai K & Kim S J, *Int J Heat Fluid Flow*, 11 (1990) 254.
10 Ishak A, Nazar R, Arifin N M & Pop I, *Int J Therm Sci*, 47 (2008) 417.
11 Rosali H, Ishak A & Pop I, *Int Commun Heat Mass Trans*, 38 (2011) 1029.
12 Chaudhary S & Kumar P, *Meccanica*, 49 (2014) 69.

13 Chaudhary S & Choudhary M K, *Indian J Pure Appl Phys*, 54 (2016) 209.
14 Shit G C, Haldar R & Mandal S, *Adv Powder Technol*, 28 (2017) 1519.
15 Bestman A R & Adjepong S K, *Astrophys Space Sci*, 143 (1988) 73.
16 Makinde O D & Ogulu A, *Chem Eng Commun*, 195 (2008) 1575.
17 Pal D & Mondal H, *Meccanica*, 44 (2009) 133.
18 Jat R N & Chaudhary S, *Z Angew Math Phys*, 61 (2010) 1151.
19 Chaudhary S, Choudhary M K & Sharma R, *Meccanica*, 50 (2015) 1977.
20 Sandeep N, Sulochana C & Rushi K B, *Eng Sci Tech An Int J*, 19 (2016) 227.
21 Chaudhary S & Choudhary M K, *Therm Sci*, 22 (2018) 797.
22 Elbashbeshy E M A & Emam T G, *Therm Sci*, 15 (2011) 477.
23 Brewster M Q, John Wiley and Sons, New York (1992).